PERMANENT ICE COVERS OF THE MCMURDO DRY VALLEY LAKES, ANTARCTICA: BUBBLE FORMATION AND METAMORPHISM

Edward E. Adams

Civil Engineering Department, Montana State University, Bozeman, Montana

John C. Priscu and Christian H. Fritsen

Department of Biological Sciences, Montana State University, Bozeman, Montana

Scott R. Smith and Steven L. Brackman

Civil Engineering Department, Montana State University, Bozeman, Montana

The permanent ice covers of liquid water based lakes in the McMurdo Dry Valleys are thermodynamically active and display a well defined but transitory stratigraphy. We discuss the annual development of the physical structure of the ice based on field measurements, data gathered during the austral winter and spring of 1994 and 1995, laboratory experiments, and quantitative analysis. In general, the ice growth takes place on the bottom of the ice cover with ablation from the top. Sediment deposited on the ice surface by aeolian processes migrates downward through the ice. The migration is driven by a combination of solar absorption and seasonal warming, leaving a liquid melt trail in its path. The sediment collects in discrete pockets forming a layer with clean ice above and below. Attenuation of solar energy coupled with the brief duration of the relatively warmer portion of the summer season limit the sediment's level of descent. During the austral summer an aquifer is created in the ice, with its lower boundary marked by the sediment layer. The aquifer is connected to the lake water through conduits and the lower ice remains essentially dry. A complex ice stratigraphy is produced as the result of top down freezing of the liquid water in the ice during fall and winter. Inverted tear-drop shaped bubbles with diameter generally under 5mm are produced in the upper meter of the ice. Arching plume-like bubbles and umbrella shaped waves of small spherical bubbles develop as the liquid freezes in the vicinity immediately above the sediment pockets. These patterns are governed by the shape of the freezing front. Liquid filled cavities in the ice induce local curvature of the freezing front, the shape of which is determined by differences in thermal conductivity of the water phases. Hoar frost, produced by temperature gradients, is apparent on the upper surfaces of many bubbles. Just below the sediment, a cluster of circular horizontal fractures develop when expansion due to the phase change of liquid entrapped in cylindrical bubbles causes failure. Fracture occurs on the basal plane of the S1 (c-axis vertical) ice. The lower region of the ice cover is characterized by vertically oriented cylindrical gas bubbles that develop when water freezes to the bottom of the ice cover. The bubbles, fractures, and sediment configuration influence light transmission/absorption, heat flux, and mass transport, all of which are important to the biogeochemical processes in the lake.

INTRODUCTION

In the Antarctic environment, the lake ice cover is a dynamic but permanent geologic structure. The ice is an essential feature influencing biologic activity in the liquid water beneath the ice cover and within a sediment layer in the ice itself [*Wing and Priscu*, 1993; *Priscu*, 1995; *Lizotte et al.*, 1995; *Fritsen et al.*, this issue]. An understanding of the physics of the ice on temporal and spatial scales will provide new information on the influence of the physical environment on the microbial populations both within the ice and in the liquid water column beneath the ice. Most of the lakes in the McMurdo Dry Valleys of Antarctica are unique in that they maintain a perennial ice cover overlying liquid water. The geomorphology and complex stratigraphy of the ice on these lakes determines the transmission, scattering and absorption of infrared and visible radiation [*Lizotte and Priscu*, 1993; *Howard-Williams et al.*, this volume]. In addition, ice shields the underlying liquid from wind induced mixing [*Spigel and Priscu*, this volume]. Ice thickness, which varies among the lakes, ranges from 3 to 6 m and is maintained by accretion on the bottom, at the liquid-ice interface. New ice formation is balanced by sublimation [*Clow et al.*, 1988] at the upper surface and melt on the bottom during the summer. The lake water is replenished by glacial melt [*Chinn*, 1993].

As early as 1966, *Henderson et al.* [1966] noted that a liquid "water table" developed within the ice cover during summer, however little research has examined the influence of the liquid water on the ice bubble morphology. *Squyres et al.* [1991] encountered liquid water 2.1 m below the surface while constructing sampling holes in Lake Hoare during November. The ice was sufficiently permeable so that the hole could not be pumped dry. They also noted that the depth at which liquid water was encountered was coincident with the bottom of in-ice sediment. *Squyres et al.* [1991] described bubble morphology within the ice hole. Some of the structure they observed has similarities to that observed in second year arctic lake ice [*Swinzow*, 1966]. *Adams et al.* [1996] noted that in a core extracted November 17, 1994 liquid was present near a sand inclusion 250 cm below the ice surface in otherwise dry ice. Within days, liquid saturated ice was encountered approximately 100 cm below the surface in the same vicinity. Liquid water ascended to the hydrostatic level of the lake after the in-ice aquifer was penetrated. Liquid water was not present at the surface so downward infiltration did not contribute to the aquifer at this time.

Ice grows in the direction of the temperature gradients that must exist at the solid-liquid interface for active freezing to occur. Vapor bubbles in the ice are the product of gas exsolution and occlusion during freezing and are oriented relative to the direction of ice growth [*Carte*, 1961; *Bari and Hallet*, 1974]. As the ice front advances downward, the solid phase rejects dissolved gases thereby increasing the supersaturation level of the liquid at the interface until, in the presence of a nucleate, a critical value for bubble formation is reached. A consequence of bubble formation is that the supersaturation of the adjacent liquid is lowered. Size, number, and shape of bubbles are to a large degree a function of ice growth rate. As the growth rate increases, the number of bubbles also increases, but the size decreases. If the growth rate of the ice and of the supersaturation of the liquid are "balanced," cylindrical bubbles will form. Waves of bubbles will form during steady freezing when the formation reduces supersaturation sufficiently to constrict the bubble; continued freezing again increases the supersaturation level causing the process to repeat.

This paper presents a physical description of the salient characteristics of the morphology of the ice structure in the permanent ice covers of lakes in the McMurdo Dry Valleys. In addition laboratory experiments that corroborate the observed morphology of in situ lake ice are described.

FIELD SITE DESCRIPTION

The McMurdo Dry Valleys of Antarctica are located at 160°–164° E, 76°30′–78°20′ S. These valleys receive precipitation on the order of 10 mm·y^{-1}, [*Bromley*, 1986] most of which is lost to sublimation. This low precipitation coupled with the continental ice sheet barrier formed by the Transantarctic Mountains produce the dry valley environment [*Chinn*, 1993]. The lakes, situated on the valley floor, are surrounded by a barren rocky/sandy mountainous landscape with alpine and continental glaciers entering from the mountainsides and along the valley floor.

We observed considerable variation of the ice covers among lakes in the McMurdo Dry Valleys with respect to sediment content, internal structure, and surface topography. Lake Vanda for example is virtually free of sediment and has a smooth surface while the ice cover at Lake Miers has large sand deposits over a meter high and a very rough ice topography. To offer a concise presentation, the discussion presented here will focus on Lake Bonney, which is intermediate among lakes with respect to sediment deposition and surface topography.

METHODS

Field

Ice cover morphology was determined largely by field studies performed during the austral spring 1994 and late winter 1995. The 1995 late winter (August–September) study provided an opportunity to examine the stratigraphy of the ice before being altered by seasonal warming.

Ice cores were obtained using a 3 inch SIPRE ice coring tool. Cores extracted during winter extended from the surface of the ice to within 50 cm of the ice-liquid inter-

face (total ice thickness 4 m). The remainder of the ice was then penetrated using an ice auger and the ice thickness measured by lowering a weighted tape measure, constructed so that it hooked onto the bottom of the ice.

Immediately upon extraction, ice cores were placed in flexible polyethylene tubing and labeled for position and orientation. A number of the samples were examined in a field laboratory on Lake Bonney where a photographic record of the morphology was made. The morphology of the ice was exposed using a warm aluminum plate to melt slightly the surface of the ice core in order to eliminate scratches left by the corer.

A second method used to examine internal structure of the ice on Lake Bonney in situ during the 1995 winter study was a 3.4 m deep pit excavated using an oil free chain saw. A hot air blower was used to melt slightly or "polish" the exposed pit wall so that the internal structure of the ice cover could be readily examined. This early season pit proved to be particularly valuable for obtaining large scale information on the ice stratigraphy. Large blocks of ice were also removed from the pit for examination.

Year round air and ice temperature data at Lake Bonney were recorded using thermocouples on a Campbell 21X data logger. They were placed in the ice at 0.5 m, 1 m, 2 m and 3.5 m below the upper surface of the ice [*Fritsen et al.*, this volume].

Laboratory

Ice was grown in a cold laboratory to examine bubble morphology resulting from downward freezing of an advancing ice front. The ice was grown in a nominal 60 cm diameter by 22 cm deep cylindrical vessel. Sides and bottom of the open container were well insulated. The vessel was placed on the floor of a –20°C cold room and immediately filled with 21°C distilled water. The ice structure for the laboratory and some of the lake ice was ascertained using cross polarized light on thin cross sections, in conjunction with polyvinyl formal crystal etching [*Higuchi and Muguruma,* 1958].

In another process, crystallographic orientated clear ice samples, used for subsequent experiments, were produced using the following laboratory procedure. Distilled water was partially degassed by boiling for 3 to 5 hours, then placed in sealed containers and cooled to approximately 1°C. The insulated container described above, which had been maintained at 21°C, was placed in the freezer and filled with the prepared water. The water was kept in still air conditions to minimize mixing from air currents, and allowed to freeze. This process produced a vertical c-axis oriented crystal structure in the ice. An average a-axis length of about 2 cm resulted. In other samples, a chilled insulated cover placed over the vessel increased the a-axis to 9 cm. The upper 15 cm of the sample yielded the bubble free ice. Samples of the clear ice approximately 20 cm long, 13 cm wide, and 10 cm deep were extracted from the top center of the larger unit.

Experiments to determine the cause of horizontal fractures observed in the lake ice were conducted using these clear oriented samples. Three 1.3 cm diameter holes were drilled to a depth of 8.5 cm into each block. The holes were used as a model of vapor cylinders observed in the Antarctic ice. Holes were drilled in the ice blocks at three different orientations: parallel with the c-axis, perpendicular to the c-axis, and oriented at 45° to the c-axis. The cylinders were filled with water using a large syringe to avoid trapping air: the sample was then frozen. Top down freezing of the liquid-filled cylinders was achieved by floating the blocks in an ice-water bath in the middle of the same insulated vessel used to grow the primary ice sample. The ensemble was then frozen in –10°C laboratory over the course of several days.

Ice specimens for studying bubble morphologies above the sediment pockets were developed by freezing water in vertically oriented transparent polycarbonate cylinders placed on an insulated platform in a cold laboratory. Dimensions of the polycarbonate freezing containers were 8.2 cm inside diameter, 0.3 cm wall thickness, and 30 cm in height. A 9 cm PVC couple securely positioned a sheet of latex rubber on the container bottom to allow for expansion of the ice. Thermal conductivities of the polycarbonate, liquid water, and ice are 0.17 $W \cdot (m°K)^{-1}$, 0.58 $W \cdot (m°K)^{-1}$, and 2.17 $W \cdot (m°K)^{-1}$ respectively.

FIELD OBSERVATIONS

A description of bubble structure, the sediment layer within the ice cover, internal fracturing, internal melting, and other features are presented in this section. This narration describes the structure from the bottom of the ice sheet upward.

In the bottom 1.5–2 m of the ice cover, vertically orientated vapor cylinders up to 20 cm long are the predominant feature. The ice in this region varies from relatively clear sections to discrete zones with a high concentration of cylindrical bubbles of varying diameter, some in excess of a centimeter (Figure 1). Larger diameter cylinders appear in conjunction with a lower concentration of bubbles.

A feature first observed during August and September 1995 is a zone of horizontal fractures. This zone is located at about 1.5 m from the bottom of the ice and consists of horizontal fractures up to 10 cm in diameter. In cross section these appear as thin horizontal planes with a string of fine vertical bubbles located near the projected center (Figure 2a). When viewed from an oblique angle the bubble strings pass through or end at the nominal centroid of a circular crack. Several of these fracture disks may be apparent along a bubble string (Figure 2b). Frequently, this line of bubbles extends upward to the longitudinal axis at the bottom of a vertical vapor cylinder (Figure 2a). Ice on the bottom of the cylinder bulges upward into the tube

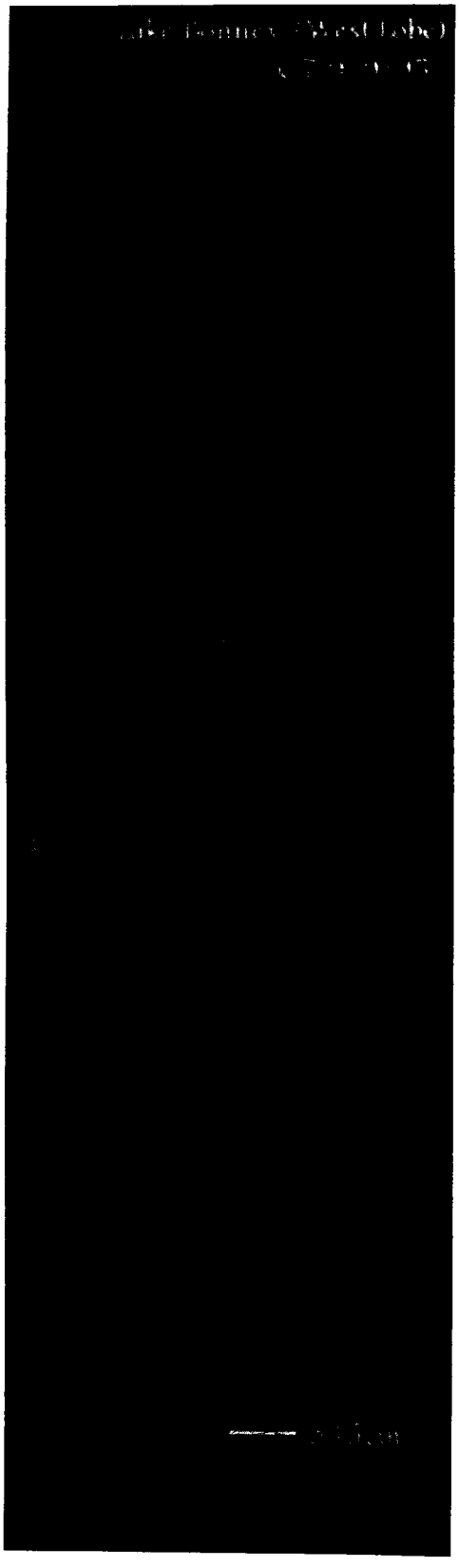

Fig. 1 Section of "3 inch" ice core (10 cm diameter) showing the vertical cylindrical bubble structure. (The horizontal cylinder apparent near the scale is an artifact of sampling.)

to form a convex ice surface. When viewed from above the fractures appear as circular white disks.

Located at about 1.6 to 2 m from the bottom of the ice cover, there is a zone of sediment composed of sand and gravel sized particles (Figure 3a). A number of former vapor cylinders have been filled with sediment in the lower region of the layer. Above the sediment filled cylinder layer is a zone where sediments form larger pockets several centimeters across. A lower concentration and smaller clusters of sediment composed of only a few sand grains occurs in the upper portion of this region.

A striking change in the structure of the bubbles occurs at the sediment layer. A few of the more distinct several patterns are presented in Figures 3b and 3c. elongated but not strictly vertical and tend to arch like pattern from the sediment pocket. Another gy consists of waves of small spherical bubbles in umbrella patterns over the sediment pocket. Plumes have been observed in excess of 30 extent (Figure 3d). Other tapering tubular bubbles along the surface of the sediment. Chains erally vertical, inverted teardrop shaped bubbles seen above the center of some of the pockets. (Color images of figures 3a through 3d, which detail, are included in the CDROM accompanying volume.)

In the region above the sediment layer and its ated bubbles, the bubbles are generally smaller an inverted teardrop shape (Figure 4a). These are with vertically oriented tubes. In the region extending the sediment layer to the top of the ice sheet, bubbles distinctly frosted on the upper surface (Figure 4c).

Figure 5 shows a sample of an ice core taken from above the sediment layer on Lake Bonney shortly liquid was first encountered in the ice (November

ANALYSIS AND LABORATORY RESULTS

Ice Growth and Gas Supersaturation

Thermocouple data from the east lobe of Lake Bonney during 1993 indicates that active ice growth will take place at the liquid-ice interface between August and November for a period of about 100 days per year (Figure 6). The rate of growth of the ice, dX/dt, is calculated from the energy equation (Figure 7) in the form

$$\rho_i L \frac{dX}{dt} = \left(k_i \frac{\partial T_i}{\partial x} - k_i \frac{\partial T_l}{\partial x}\right) \qquad (1)$$

Figure 2a

3. Horizontal fractures and thin bubble train which occur in ...ants of the vertical cylindrical vapor bubbles Fractures are ... result of stresses produced by trapped liquid water expansion ... to freezing. Note also the concave lower surface of the ...ining portion of the vapor cylinder (a). A series in of frac... are produced due to stress relief as a result of the ice failure ...owed by continued freezing (b).

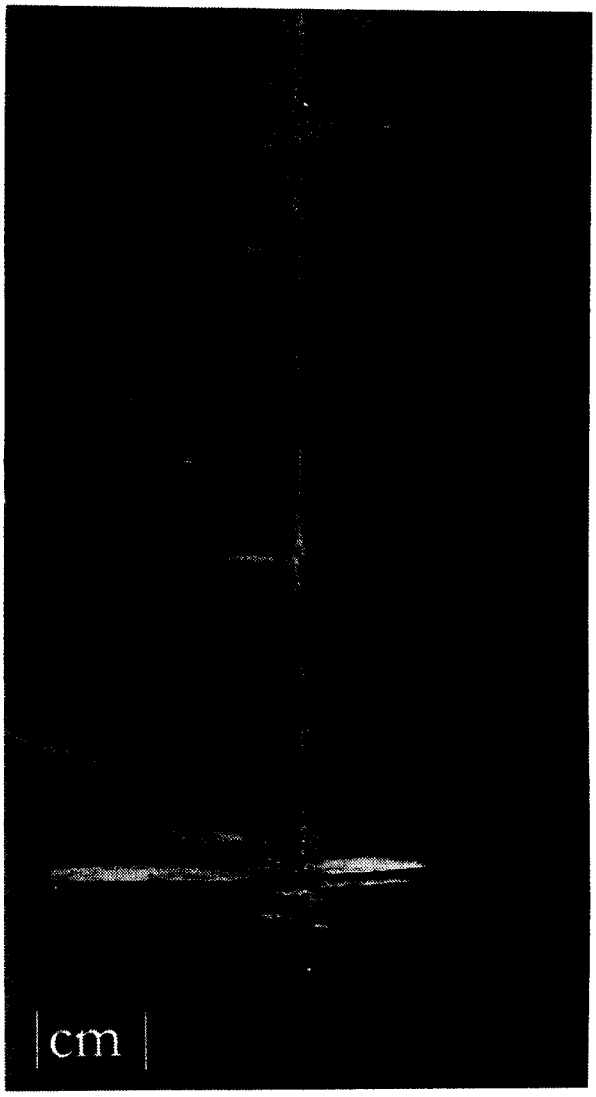

Figure 2b

...ere the subscripts i and l represent ice and liquid, t is ...e, k is the thermal conductivity, T is temperature, ρ is ...e density, and L is the heat of phase change. Assuming a ...emperature gradient in the liquid of 0.5°C·m^{-1} and an ice ...ickness of 3.9 m at the start of the growth period, this ...odel predicts ice growth of about 3.5 mm d^{-1} (Figure 7) ...between August and November.

As the ice surface advances during freezing and re...jects vapor into the liquid at the ice surface, a gas concen...tration gradient normal to the ice surface develops. The governing equation describing the ratio of gas concentration to some initial value as a function of time, t, and position, x, in the fluid ahead of the moving ice front is given as [*Carte*, 1961]

$$\frac{C(x,t)}{C_o} = 1 + \frac{1-\xi}{\xi}\{exp(-\frac{Rx}{D}) \ldots$$

$$- exp[-\frac{R}{D}(1-\xi)(x+\xi Rt)]\} \quad (2)$$

where C is the solute concentration, C_o is the initial solute concentration, D is the diffusivity of air in water, x is the distribution coefficient (ratio of solute air in the solid and liquid), and R is the freezing rate of the interface. To illustrate the development of air supersaturation in water at the interface we examine a constant ice growth rate of 3.5

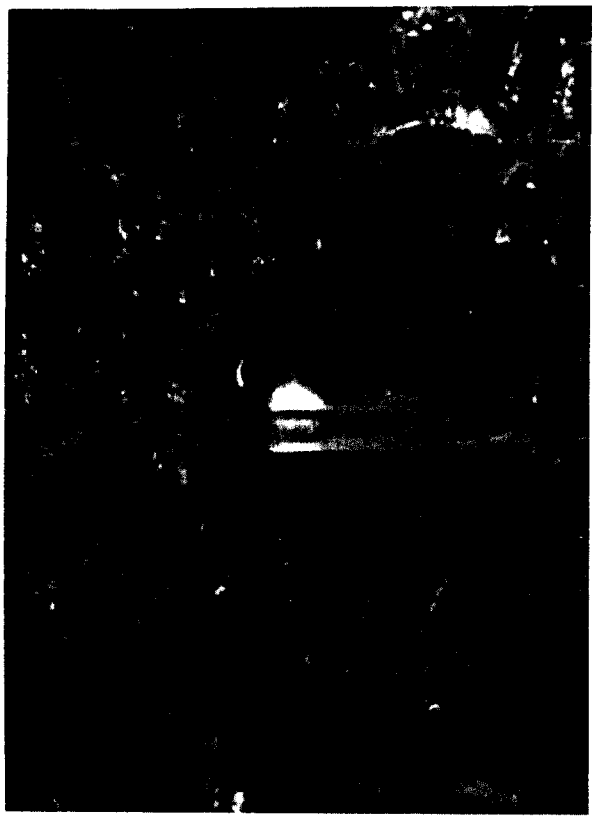

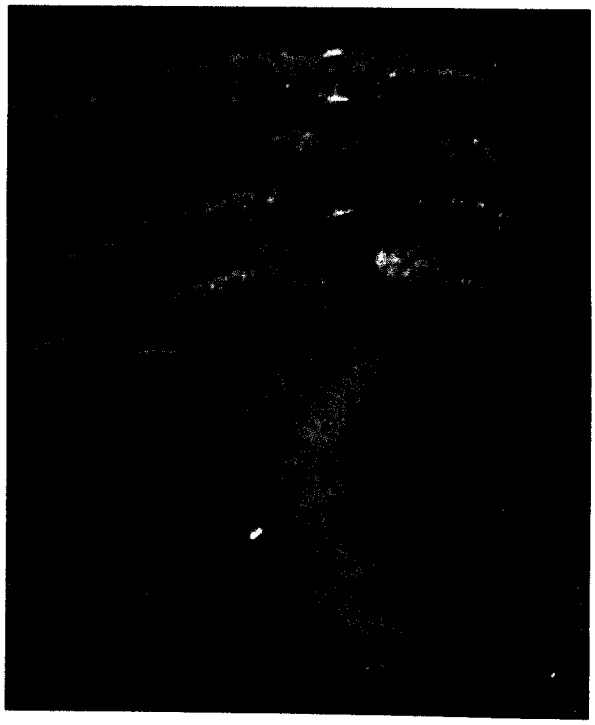

Figure 3b

Figure 3c

Fig 3. Sediment layer which is located about 1.5 to 2 cm from the bottom of the 4 cm ice cover on Lake Bonney. It is composed predominantly sand sized particles (a). Complicated vapor bubble morphology such as these bubble chains and plume-like bubbles develop directly above sediment pockets in the lake ice (b). Arching wave of umbrella shaped bubbles (c).

mm·d-1 (based on results shown in Figure 6). The concentration ratio would increase 12 fold, as shown for 30 cm of ice growth (Figure 8), owing largely to the slow diffusion through the liquid. This increase does not account for the development of bubbles which would lower the calculated values. It should also be noted that the lake water is in an initial state of supersaturation. In addition, even slight convection with respect to oxygen and nitrogen that may occur in the lake would lower the concentration at the interface.

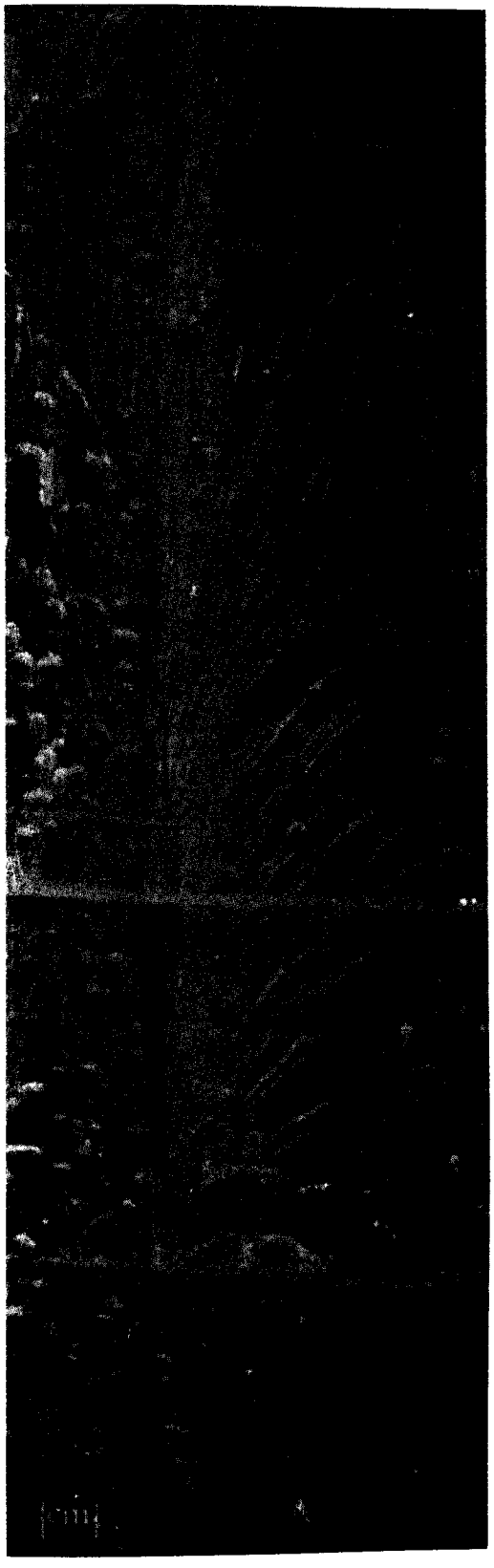

Laboratory Bubble Formation

Insulative properties of the polycarbonate cylinders used to examine the sediment related bubble morphology caused the top of the water exposed to the air to freeze first. The combined components of vertical and horizontal heat flux then produce a curved freezing front. Alteration of thermal properties as the result of the phase change further influences the heat flux, contributing to the development of a concave downward circular paraboloid as the freezing front. Figure 9 illustrates a progression of the freezing front in a vessel held at an ambient room temperature of –7°C. Note the parabolic freezing front that produces the arching bubble shapes, the vertical linear front that develops horizontal cylindrical morphologies, and the bubble chains that develop near the top center. The development of a circular paraboloid at the freezing front was common to all samples which were frozen in the 8 x 30 cm polycarbonate containers at temperatures of 0°C, –7°C, and –23°C.

The plume-like bubble patterns developed in these experiments for ambient laboratory temperatures of 0°C and –7°C but not at –27°C. The plume shape was observed to develop normal to the curved path of the advancing ice front. Nearly horizontal cylindrical bubbles developed on the sides at depth following the nearly vertical orientation of the freezing front in this region. This pattern is similar to the vertically oriented cylindrical bubbles that develop at the flat horizontal freezing front in the lake ice and in the large laboratory vessel. Some of the large arching cylindrical bubbles exhibit ridges on the top surface, a characteristic similar to that observed in some of the lake ice. The largest cylindrical and plume like bubbles developed when the ambient laboratory temperature was near 0°C, inducing a slow growth rate.

Bubble chains in the laboratory ice were located near the top center of the sample cylinder (Figure 10a) interior to the arching and horizontal cylindrical bubbles, and were most pronounced at the slower freezing rates. Bubble chains develop when the ice front is encroaching on the center and the gas concentration increases accordingly. The mechanism of formation is presumably similar to that described by *Carte* [1961] for the waves of bubbles. Bubbles forming near the bottom of the test cylinder were observed to detach and buoyantly ascend to the vertex of the parabaloid during laboratory experiments, contributing to bubble formation at that location.

A cloud of small spherical bubbles developed when the freezing rate was increased in the presence of lower ambient laboratory temperature (–27°C). These clouds appear similar to those observed just above the sediment in in the lake ice (Figure 3c). Like bubble chains, cloud bursts appear in the center of the frozen sample. The higher freezing rate results in the large number of small bubbles.

Figure 3d

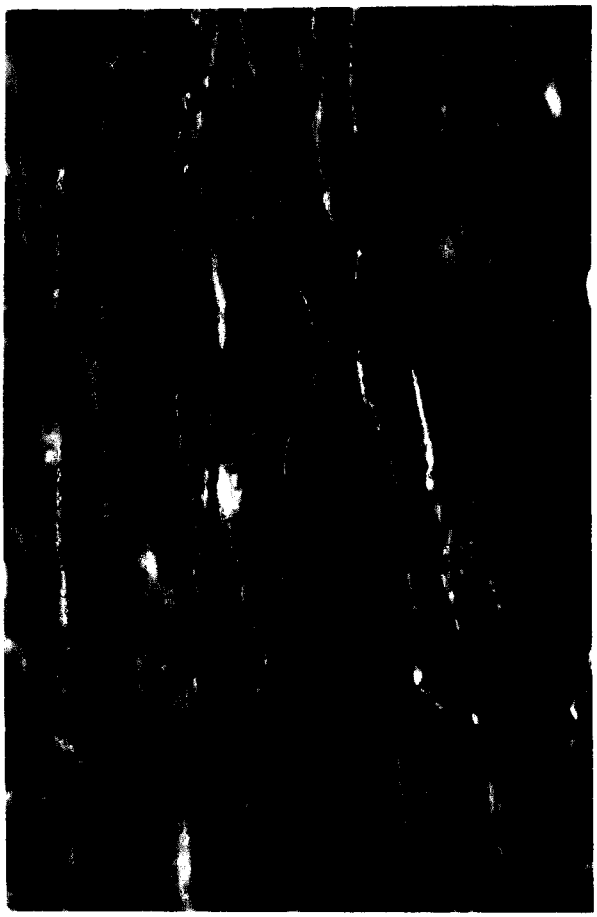

Figure 4a

Figure 4b

Fig. 4 Inverted teardrop and fine tube-like bubbles predominate in the upper regions of the ice cover . The largest bubble in the figure is about 2 mm (a). Frost on the top surfaces is coarse. The result of sublimation and condensation across the fabric driven by a strong temperature gradient (b).

Umbrella shaped bubble waves (Figure 10b) formed in the laboratory when the vertical walls of the polycarbonate cylinder were wrapped with additional insulation, reducing the horizontal component of freezing. As the curved freezing front advanced, a layer of small spherical bubbles formed, following the contour of the freezing front. The formation of small bubbles presumably lowered gas supersaturation and clearer ice followed until the liquid water again became supersaturated with gas resulting in another wave of bubbles.

These laboratory results are essentially qualitative and were conducted to gain insight into probable physical constraints that would cause the formation of the complex bubble structure observed in the lake ice. In this regard, the experimental results were successful. Morphologies similar to those observed in the lake ice have been reproduced and potential mechanisms that would lead to appropriate boundary conditions are identified in the following section.

Horizontal Fractures

Water frozen in the large vessels, as described in the laboratory methods above, initially forms a cap of ice across the top, trapping dissolved gasses in the liquid below. In cross section, the top 15 cm of the laboratory ice is clear but transitions below to predominantly vertical cylindrical bubbles. Interspersed among the cylinders were occasional chains of teardrop shaped bubbles with the tapered end pointing downward.

Several methods of freezing the liquid which filled the holes drilled in the clear crystal oriented ice samples were investigated to examine the consequence of the manner of freezing. Water injected into the holes of a block which had come to thermal equilibrium with the −10°C cold room froze within seconds. A large number of very small scattered bubbles developed in the ice filled hole, but no cracking occurred. Three other samples were brought to approximately 0°C, and the holes filled with water. The tops of

5 An ice core taken when liquid water was present in the This appears to be a remnant of plume-like bubble. Water drained from the sample.

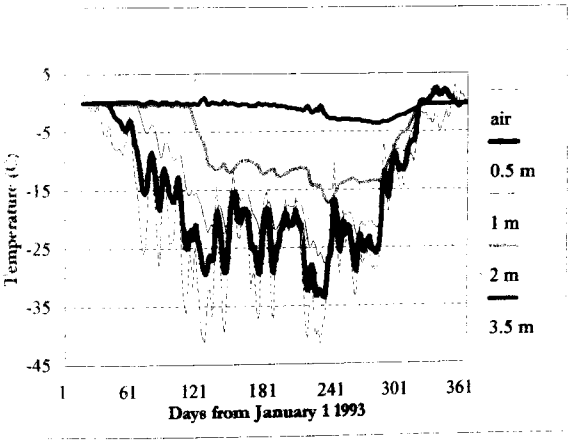

Fig. 6 Temperature profile for Lake Bonney, 1993.

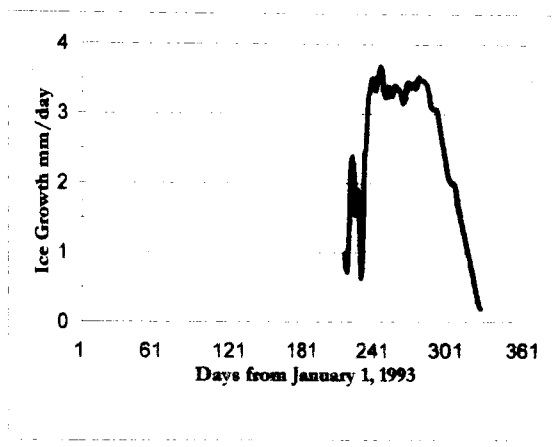

Fig. 7 Calculated ice growth to the bottom of the ice sheet based on thermocoule data for Lake Bonney, 1993.

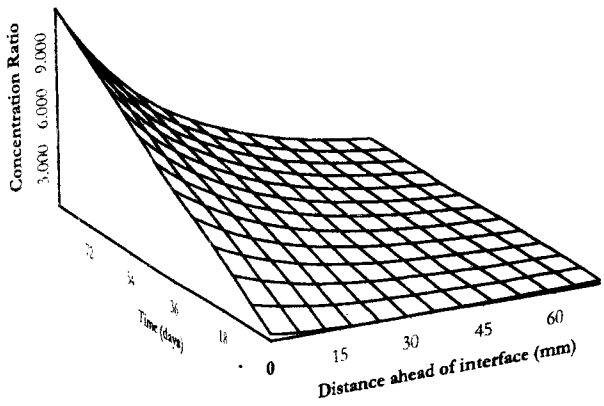

Fig. 8 An example of the supersaturation increase in the liquid at the freezing front for ice to grow 30 cm (about 86 days) at a rate of 3.5 mm·d-1.

the holes of two were sealed by freezing with a −10°C aluminum plate. Individual samples placed in a −10°C and a −2°C environment produced cracking in each but no orientation was apparent. The third block was placed in the −2°C environment without sealing the top. No cracking was induced in this case.

In each laboratory specimen subjected to the predominant top down freezing process described above, a well defined circular fracture occurred on the basal plane. The basal plane is orthogonal to the c-axis of the ice crystal. This was consistent for the samples composed of large and small crystals and in the case where a hole was placed in a single crystal, regardless of the orientation of the crystal axis relative to the direction of freezing. The basal plane

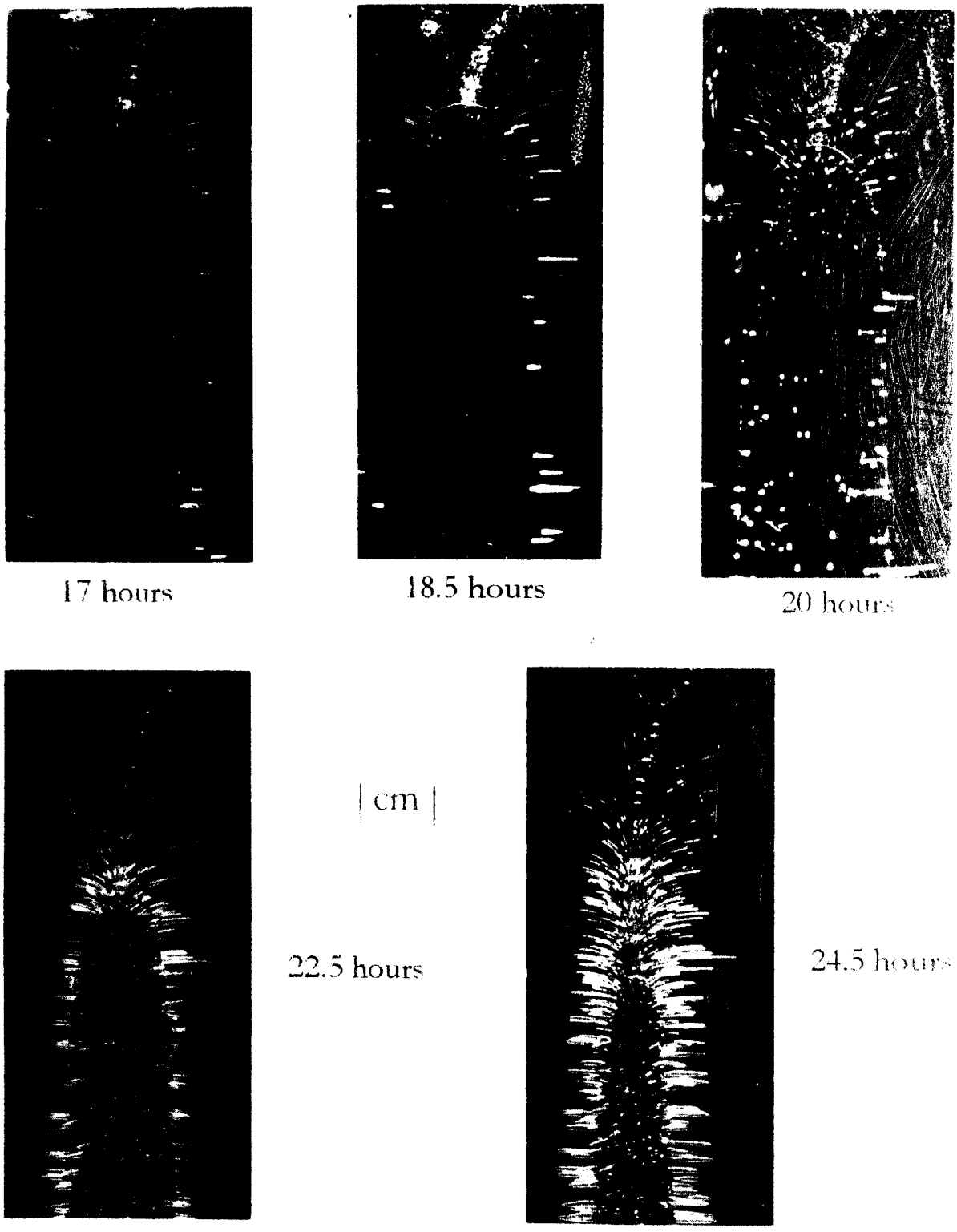

Fig. 9 Time lapse images of ice growing at –7°C in an 8 x 30 cm polycarbonate cylinder. Note the parabolic shape of the freezing front as the ice advances downward and inward. Bubble structure is oriented normal to the freezing front.

Figure 10a

Figure 10b

Fig. 10. Laboratory grown bubble chain and plume like structure (a). Laboratory grown waves of umbrella patterned small spherical bubbles (b).

failure for the vertically oriented crystal structure is similar to that observed in the lake ice (see Figures 5a and 5b), i.e., a thin line of bubbles developed on the central vertical axis of each refrozen cylinder.

Horizontal fractures in the essentially vertically oriented c axis lake ice are hypothesized to be the result of hydrostatic pressure induced by the volumetric increase from phase change during top down freezing. An analysis describing the influence on fracturing due to volumetric expansion during solidification is presented. Water expands upon solidification, therefore downward freezing in the cylindrical hole causes compression of the fluid trapped below, producing a rise in the hydrostatic pressure. This pressure then induces a stress field in the surrounding ice which may lead to failure.

Ice with a crystallographic orientation exhibits orthotropic behavior, governed by its crystal structure, whereby (depending on loading conditions) it will tend to fail along its basal plane due to shearing stress [*Michel*, 1978]. *Michel* [1978] found that a specimen of ice loaded in uniaxial tension or compression, regardless of the loading orientation with respect to the basal plane, always failed along the basal plane of S1 ice in shear, except at the extremes when the basal plane is parallel or normal to the direction of a uniaxial load. *Ashton* [1986] reported a range of 0.2 to 4.0 MPa for shear strength of ice.

In the case of downward freezing of the liquid filled cylinder, the increased pressure in the entrapped fluid is examined by considering the equation for the bulk modulus, κ, of a fluid at constant temperature, T.

$$\kappa = -V\left[\frac{\partial p}{\partial V}\right]_T \tag{3}$$

where p is pressure and V is volume. The negative sign indicates that as pressure increases volume decreases. Rearranging this equation and expressing it in terms of finite values yields,

$$\Delta P = \kappa\frac{-\Delta V}{V_o} \tag{4}$$

where V_o is the initial fluid volume. For the sake of our discussion, if we consider 4.5 cm of the original 8.5 cm

long (1.27 cm diameter) hole used for the laboratory study to have frozen, an unconfined expansion of 0.47 cm^3 would result (assuming the density ratio of ice to water as 0.917). Neglecting visco-elastic deformation of the ice this gives $\Delta V = -0.47$ cm^3 and an unconfined initial volume, $Vo = 5.54$ cm^3. Using $\kappa = 1964$ MPa for water at 0°C, the increase in pressure is calculated to be $\Delta P = 178$ MPa. By similar analysis, if 2.5 cm in this example had frozen then the pressure would be 70 MPa; freezing 6.5 cm would yield 443 MPa.

This increase in pressure in the fluid induces stress in the surrounding ice. Principal stresses in a thick walled pressure vessel may be calculated in cylindrical coordinates [e.g., *Boresi and Sidebottom*, 1993] using the set of equations,

$$\sigma_{rr} = \frac{p_1 a^2 - p_2 b^2}{b^2 - a^2} - \frac{a^2 b^2}{r^2 (b^2 - a^2)} (p_1 - p_2)$$

$$\sigma_{\theta\theta} = \frac{p_1 a^2 - p_2 b^2}{b^2 - a^2} + \frac{a^2 b^2}{r^2 (b^2 - a^2)} (p_1 - p_2)$$

$$\sigma_{zz} = \frac{p_1 a^2 - p_2 b^2}{b^2 - a^2} \qquad (5)$$

where σ indicates normal stress and the subscripts imply cylindrical coordinate directions (radial, angular, vertical), a and b are, respectively, the inner and outer diameters of the cylinder, p_1 and p_2 are the internal and external pressures and r is the radial distance to the point of interest. To calculate the increase in stress, ΔP is used for p_1, and p_2 is taken as 0, $a = (1.27/2)$ cm, $b = 30$ cm (the radius of the container in which the sample is centered). Values are calculated at $r = a$ where the ice stress will be a maximum. Using the values discussed above, this yields values for stress of $\sigma_{rr} = -p = -178$ MPa (compression), $\sigma_{\theta\theta} = p = 178$ MPa (tension), and $\sigma_{zz} = 2.0$ MPa (tension). The maximum shearing stress will occur on a plane oriented at 45° to the maximum and minimum normal stresses. In this case $\sigma_{\theta\theta}$ and σ_{rr} are the maximum and minimum values so the maximum shearing stress is oriented on a plane at 45° to the ρ–θ axes. The maximum shear stress, τ_{max}, is found from

$$\tau_{max} = \frac{\sigma_{max} - \sigma_{min}}{2} \qquad (6)$$

which yields of $\tau_{max} = 178$ MPa for the example under discussion.

In the ideal case of perfectly vertical c-axis crystals and perfectly vertical cylindrical holes, no shear stress would be generated on the basal plane. However if a crystal orientation is rotated about the r coordinate relative to the vertical by an amount ϕ, the shear stress may be computed on this plane using the equation,

$$\tau_{\theta z} = \frac{\sigma_{\theta\theta} - \sigma_{zz}}{2} \sin(2\phi) + \tau_{\theta z} \cos(2\phi) \qquad (7)$$

It would require that a slight off vertical orientation of less than 1 degree of the crystal c-axis would be sufficient to induce shear stress failure in the range reported in the literature [*Ashton*, 1986]. Results from our laboratory experiments and analysis support the contention that horizontal fractures observed in the lake ice are the result of expansion caused by downward freezing of liquid water that has infiltrated cylindrical bubbles.

DISCUSSION AND CONCLUSIONS

Figure 11 presents the spatial and temporal interaction of the processes inherent to the ice covers of the McMurdo Dry Valley lakes. The relationship between mechanisms in the atmosphere, the ice cover and the liquid lake water are shown as seasonal transition between the wet summer months and the dry winter months.

The near surface bubble morphology within the ice in the ridge and troughs differ. Ice in the ridges is more porous than the ice at the trough surface that results from freezing of summer surface melt ponding in depressions. The topology of the ridges provides more surface exposure to the atmosphere, which coupled with its higher porosity ice will likely cause a higher ablation rate of the ridge ice.

During the summer months, sediments absorb solar radiation forming liquid water pockets. Although most of the vertical elongate bubbles remain dry, liquid water infiltrates those just below the sediment layer. Liquid lake water is connected to the sediment layer via vertical cracks in the ice cover. As winter approaches, top down freezing produces teardrop shaped bubbles in the upper region and plume shaped bubbles, umbrella waves, and bubble clouds above the sediment pockets. Temperature gradients across the bubbles produce hoar frost in the teardrop shaped bubbles, which greatly increases light attenuation through the ice. The liquid water that drains into and partially fills the elongate bubbles freezes, producing disk shaped horizontal fractures. The deeper elongate bubbles remain dry and unaffected by the summerwinter transition. Sediment is presumably lost from the ice cover through the vertical cracks in the ice cover. This contention is supported by large discrete sediment piles that have been observed on the bottom of the lakes [*Squyres et al.*, 1991].

It is likely that the liquid water in the summer aquifer eventually saturates the ice from the sediment layer up to the hydrostatic lake level. The morphology in the core sample in Figure 5 indicates that the liquid is penetrating a plume-like vapor inclusion characteristic of those above the sediment. Penetration of this sort increases the liquid water permeability of the ice as the in-ice aquifer develops.

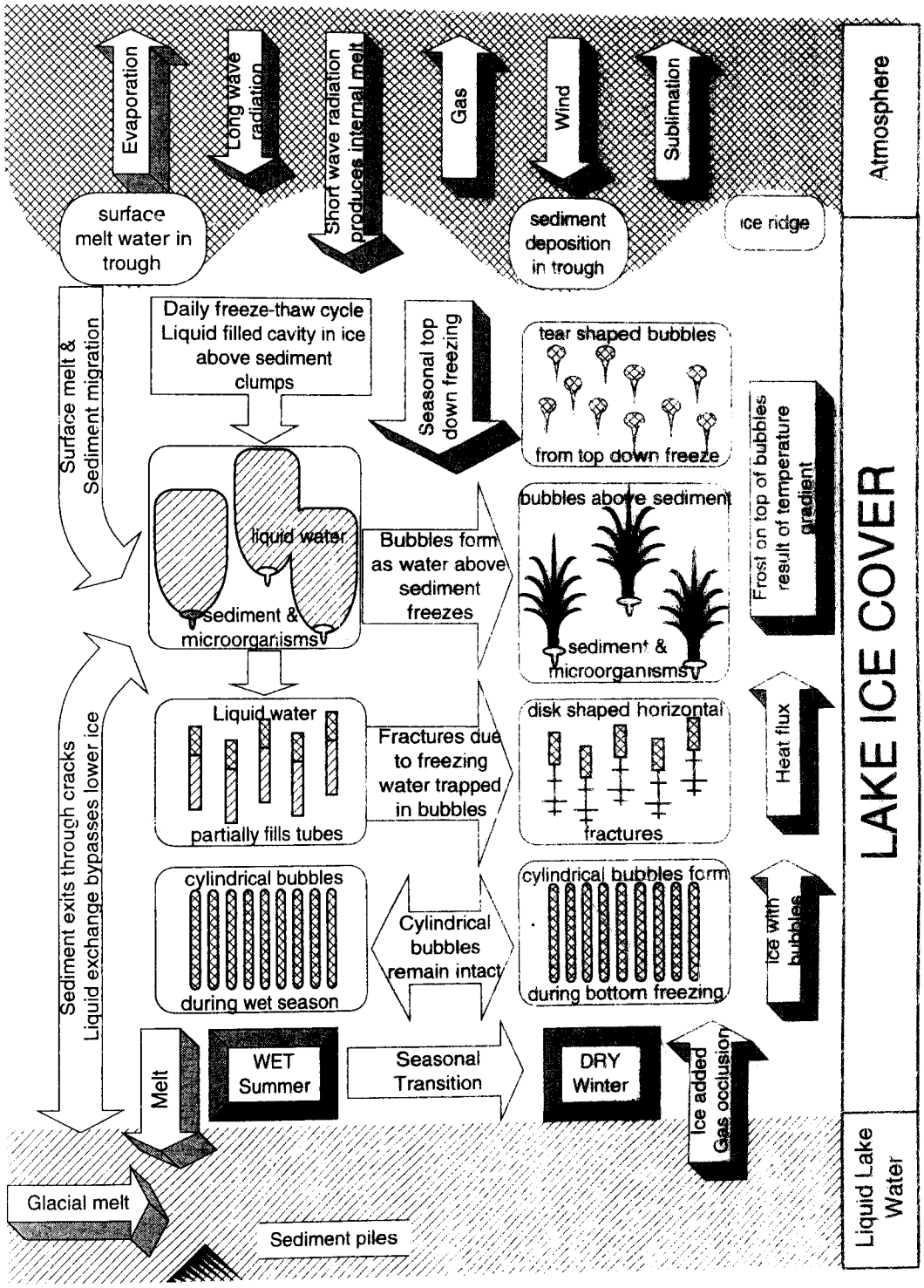

Fig. 11 A conceptual model of the temporal and spatial veriation of the ice cover. Liquid water in the ice cover which develops in the summer months plays a predominant role in the structure of the ice morphology during top down winter freezing. Cylindrical bubble develop from the freezing of lake water at the bottom.

Craig et al. [1992] contend that gas bubbles are a mechanism for the transfer of gas from lake water to the atmosphere. *Craig et al.* [1992] assumed that gas in bubbles formed at the bottom of the ice cover is carried with the ice as it gradually works upward to the ablating surface. This process has also been considered by *Priscu* [1997] and *Priscu et al.* [1996] as a mechanism for the transport of gas from lake water to the atmosphere. Our data show that the *Craig et al.* [1992] scenario is valid for the portion of the ice only below the sediment layer i.e., where the cylindrical bubbles exist, but would not account for the gas transported through the liquid water conduits, or in the region above the sediment. It is likely that when the summer ice is liquid saturated this water is in communication with the atmosphere and presumably will have equilibrium values of the dissolved gases.

Minerals, nutrients, and microbes associated with aeolean sediments migrate through the ice where a portion may enter the water column and the lake bottom. Calculations by *Simmons et al.* [1987], in an examination of the warming of subsurface ice to the melting point, indicate that solar absortion would be ineffective to cause melt for −1°C ice unless the sand particles were very large. However when we consider that in the warmer months the ice becomes isothermal at 0°C (see Figure 6), the amount of energy required to facilitate this process is much lower. The equation used by *Simmons et al.* [1987] indicates that, if all other variables are held constant, the radius of the particle varies linearly with the temperature difference between the sediment particle and the ice, with the particle size going to zero as the temperature difference approaches zero.

The continuity of the bubbles in the lake ice just above the sediment zone implies a previous equivalent continuity of the liquid phase in the ice. We believe that a situation exists in which the large volume of liquid water in the aquifer above the sediment layer occurs in pockets formed by the downward sediment migration moving through the liquid-saturated ice, assisted in its descent by absorbing solar radiation. Melt paths result with the sediment pockets at the bottom. We demonstrated in the laboratory that neither sediment nor microbes need be present to form the over sediment bubble morphology, but a mechanism is necessary for controlling the direction of the freezing front. If a liquid filled cavity above the sediment is produced then a situation similar to the laboratory experiments we described would exist, whereby the higher conductivity of the ice would cause a curved freezing front leading to the shapes observed in the lake ice.

In addition to exsolution of gases due to freezing, microbes active when liquid water is available at the sediment layer [*Wing and Priscu*, 1993] produce gas as the byproduct of biologic processes. Although these biologically generated gasses are not required for the development of bubbles in the ice, they can contribute to the supersaturation level and thus modify the bubble morphology in their immediate proximity. Since the presence of the bubbles strongly influences the manner in which light is scattered the microorganisms can contribute to the physical structure of their niche in the ice. Although additional investigation is warranted, the bubble structure will influence the manner in which the light energy will be made available to the absorptive sediment and the microbes, many of which are photoautotrophs [*Wing and Priscu*, 1993]. This concept is particularly intriguing when coupled with the reflection from the horizontal fractures, in that it offers the possibility of additional energy for melt and photosynthesis. Hence a situation may exist where the physical structure of the ice can benefit microorganisms that have been observed to grow in association with the lake ice sediment layer.

REFERENCES

Adams, E. E., J. C. Priscu, and A. Sato, Some Metamorphic Processes in Antarctic Lake Ice. *Antarctic Journal of the United States*, 1996.

Ashton, G. D, *River and Lake Ice Engineering*. Water Resources Publications, Littleton, Colorado, U.S.A. 1986.

Bari, S. A. and J. Hallett, Nucleation and Growth of Bubbles at An Ice-Water Interface. *Journal of Glaciology*. 13(69), 489-520, 1974.

Boresi, A. P. and O. M. Sidebottom, *Advance Mechanics of Materials*, Fifth Ed., John Wiley & Sons, New York, 1993.

Bromley, A.M., Precipitation in the Wright Valley, N.Z. *Antarctic Record*, Special Supplement, 6, 60–68, 1986.

Carte, A. E., Air Bubbles in Ice. *Proceedings of the Physical Society* (London), 77(495),757–768, 1961.

Chinn, T. J., Physical Limnology of the Dry Valley Lakes in *Physical and biogochemical processes in Antarctic lakes*. Antarctic Research Series, vol. 59, edited by W. J. Green and E. I. Friedman, 1–51, 1993.

Clow, G. D., C. P. McKay, G. M. Simmons, and R. A. Wharton Jr., Climotological Observations and Predicted Sublimation Rates at Lake Hoare, Antarctica. *Journal of Climate* , 1988

Craig, H, R.A. Wharton, and C. P. Mckay, Oxygen Supersaturation in Ice Covered Antarctic Lakes: Biological Versus Physical Contributions. *Science*, 255,318–321, 1992.

Fritsen, C. H., E. E. Adams, C. P. McKay, and J. C. Priscu, Permanent Ice Covers of the McMurdo Dry Valley Lakes, Antarctica: Liquid Water Content, this volume

Henderson, R.A., W.M. Prebble, R.A. Hoare, K.B. Popplewell, D.A. House, and A.T. Wilson, An ablation rate for Lake Fryxell, Victoria Land, Antarctica. *Journal of Glaciology*, 6, 129–133, 1966.

Higuchi, K and J. Muguruma, Etching of ice crystals by the use of plastic replica film, *Journal of the Faculty of Science*, Hokkaido University, Japan, Ser VII, 1(2),81–91 1958.

Howard-Williams, C., A.-M. Schwarz, I. Hawes, and J.C. Priscu. Optical properties of the McMurdo Dry Valley Lakes, Antarctica, this volume

Lizotte, M.P. and J.C. Priscu. Spectral irradiance and bio-optical properties in perennially ice-covered lakes of the dry valleys (McMurdo Sound, Antarctica). *Antarctic Res. Ser.* 57:1–14, 1992.

Lizotte, M.P., T.J. Sharp, and J.C. Priscu. Phytoplankton dynamics in the stratified water column of Lake Bonney, Antarctica: I. Biomass and productivity during the winter-spring transition. *Polar Biology*, In Press

Michel, B., *Ice Mechanics*. Les Presses De LíUniversite Laval, Quebec, 1978

Priscu, J.C. Phytoplankton nutrient deficiency in lakes of the McMurdo Dry Valleys, Antarctica. *Freshwater Biology,* In Press, 1995.

Priscu, J. C., M. T. Downes, and C. P. McKay. Extreme supersaturation of nitrous oxide in a poorly ventilated Antarctic lake. *Limnology and Oceanography*, 1996.

Priscu, J.C., The Biogeochemistry of nitrous oxide in permanently ice-covered lakes of the McMurdo Dry Valleys, Antartica in *Global Change Biology Special Issue, Microbially Mediated Atmospheric Change* (J. Prosser, ed.), 1997.

Simmons, G. M. Jr, R. A. Wharton Jr., C. P. McKay, S. S. Nedell, and G. Clow, Sand/ice interactions and sediment deposition in perenially ice-covered Antarctic Lakes, *Antarctic Journal of the United States*, 237–240, 1987.

Spigel, R.H. and J.C. Priscu, Physical limnology of the McMurdo Dry Valley Lakes, this volume.

Squyres, S. W., D. W. Anderson, S. S. Nedell, and R. A. Wharton, Lake Hoare, Antarctica: sedimentation through a thick perennial ice cover. *Sedimentology*, 38, 363–379, 1991.

Swinzow, G. K., Ice cover of an arctic proglacial lake. *U. S. Army Cold Regions Research and Engineering Laboratory (USA CRREL), Research Report* 155, 1966.

Wing, K. T. and J. C. Priscu, Microbial communities in the permanent ice cap of Lake Bonney, Antarctica: Relationships among chlorophyll-*a*, gravel, and nutrients. *Antarctic Journal of the United States*, 28: 246–249, 1993.

E. E. Adams, Civil Engineering Department, Montana State University, Bozeman, MT, 59717

S. L. Brackman, Civil Engineering Department, Montana State University, Bozeman, MT, 59717

C. H. Fritsen, Department of Biological Sciences, Montana State University, Bozeman, MT, 59717

J. C. Priscu, Department of Biological Sciences, Montana State University, Bozeman, MT, 59717

S. R. Smith, Civil Engineering Department, Montana State University, Bozeman, MT, 59717

(Received December 13, 1996;
accepted April14, 1997.)